



# Endothelial *BMPR2* Loss Drives a Proliferative Response to BMP (Bone Morphogenetic Protein) 9 via Prolonged Canonical Signaling

Anne L. Theilmann, Lindsey G. Hawke, L. Rhiannon Hilton, Mara K.M. Whitford, Devon V. Cole, Jodi L. Mackeil, Kimberly J. Dunham-Snary, Jeffrey Mewburn, Paula D. James, Donald H. Maurice, Stephen L. Archer<sup>1D</sup>, Mark L. Ormiston

**OBJECTIVE:** Pulmonary arterial hypertension is a disease of proliferative vascular occlusion that is strongly linked to mutations in *BMPR2*—the gene encoding the BMPR-II (BMP [bone morphogenetic protein] type II receptor). The endothelial-selective BMPR-II ligand, BMP9, reverses disease in animal models of pulmonary arterial hypertension and suppresses the proliferation of healthy endothelial cells. However, the impact of *BMPR2* loss on the antiproliferative actions of BMP9 has yet to be assessed.

**APPROACH AND RESULTS:** BMP9 suppressed proliferation in blood outgrowth endothelial cells from healthy control subjects but increased proliferation in blood outgrowth endothelial cells from pulmonary arterial hypertension patients with *BMPR2* mutations. This shift from growth suppression to enhanced proliferation was recapitulated in control human pulmonary artery endothelial cells following siRNA-mediated *BMPR2* silencing, as well as in mouse pulmonary endothelial cells isolated from endothelial-conditional *Bmpr2* knockout mice (*Bmpr2<sup>EC-/-</sup>*). BMP9-induced proliferation was not attributable to altered metabolic activity or elevated TGF $\beta$  (transforming growth factor beta) signaling but was linked to the prolonged induction of the canonical BMP target *ID1* in the context of *BMPR2* loss. In vivo, daily BMP9 administration to neonatal mice impaired both retinal and lung vascular patterning in control mice (*Bmpr2<sup>EC+/+</sup>*) but had no measurable effect on mice bearing a heterozygous endothelial *Bmpr2* deletion (*Bmpr2<sup>EC+/-</sup>*) and caused excessive angiogenesis in both vascular beds for *Bmpr2<sup>EC-/-</sup>* mice.

**CONCLUSIONS:** *BMPR2* loss reverses the endothelial response to BMP9, causing enhanced proliferation. This finding has potential implications for the proposed translation of BMP9 as a treatment for pulmonary arterial hypertension and suggests the need for focused patient selection in clinical trials.

**GRAPHIC ABSTRACT:** A [graphic abstract](#) is available for this article.

**Key Words:** angiogenesis modulating agents ■ bone morphogenetic protein receptors, type II ■ endothelial cells ■ growth differentiation factor 2 ■ hypertension, pulmonary ■ inhibitor of differentiation protein 1 ■ lung

Pulmonary arterial hypertension (PAH) is a fatal disease that is marked by the cancer-like proliferation of pulmonary vascular smooth muscle and endothelial cells.<sup>1</sup> This pathological vascular remodeling leads to occlusion of the precapillary pulmonary arteries, increased pulmonary vascular resistance, right ventricular hypertrophy, and death due to right heart failure within 3 years of diagnosis if left untreated.<sup>2</sup> Germline loss-of-function mutations in *BMPR2*—the gene encoding

the BMPR-II (BMP [bone morphogenetic protein] type II receptor)—have been identified in  $\approx 20\%$  of all PAH cases and over 70% of inherited disease.<sup>3,4</sup> These mutations raise an individual's risk of developing PAH by  $\approx 20\,000$ -fold, from 10 to 15 per million in the general population<sup>5,6</sup> to a disease penetrance of 27% among mutation carriers.<sup>7</sup> Although the heterozygous nature of PAH-associated *BMPR2* mutations should theoretically cause a 50% reduction in BMPR-II receptor levels, cells

Correspondence to: Mark L. Ormiston, PhD, Department of Biomedical and Molecular Sciences, Queen's University, Room A209, Botterell Hall, 18 Stuart St, Kingston, Ontario K7L 3N6, Canada. Email [mark.ormiston@queensu.ca](mailto:mark.ormiston@queensu.ca)

The Data Supplement is available with this article at <https://www.ahajournals.org/doi/suppl/10.1161/ATVBAHA.119.313357>.

For Sources of Funding and Disclosures, see page 2617.

© 2020 The Authors. *Arteriosclerosis, Thrombosis, and Vascular Biology* is published on behalf of the American Heart Association, Inc., by Wolters Kluwer Health, Inc. This is an open access article under the terms of the [Creative Commons Attribution Non-Commercial-NoDerivs](#) License, which permits use, distribution, and reproduction in any medium, provided that the original work is properly cited, the use is noncommercial, and no modifications or adaptations are made.

*Arterioscler Thromb Vasc Biol* is available at [www.ahajournals.org/journal/atvb](http://www.ahajournals.org/journal/atvb)

## Nonstandard Abbreviations and Acronyms

<b>Alk1</b>	activin receptor-like kinase 1
<b>BMP</b>	bone morphogenetic protein
<b>BMPR-II</b>	bone morphogenetic protein receptor 2
<b>BOEC</b>	blood outgrowth endothelial cell
<b>ECAR</b>	extracellular acidification rate
<b>EGM</b>	endothelial growth media
<b>HPAEC</b>	human pulmonary artery endothelial cell
<b>Id</b>	inhibitor of DNA binding/inhibitor of differentiation
<b>IL</b>	interleukin
<b>MPEC</b>	mouse pulmonary endothelial cell
<b>OCR</b>	oxygen consumption rate
<b>P</b>	postnatal day
<b>PAH</b>	pulmonary arterial hypertension
<b>TGF<math>\beta</math></b>	transforming growth factor beta
<b>TNF</b>	tumor necrosis factor alpha
<b>WT</b>	wild type
<b>ZsGreen</b>	zoanthus sp. green

and tissues from PAH patients typically exhibit a mean reduction of  $\approx 75\%$ , with some patients exhibiting a near-complete loss of BMPR-II protein.<sup>8,9</sup> Similar reductions in BMPR-II protein have been reported in PAH patients with and without *BMPR2* mutations, further supporting a critical role for BMPR-II loss and impaired BMP signaling in disease pathogenesis, independent of etiology.<sup>8,9</sup>

Although *BMPR2* is expressed in various tissues throughout the body, multiple studies point to the pulmonary endothelium as the cell type that is most critically impacted by BMPR-II loss in PAH.<sup>10–13</sup> Endothelial cells from PAH patients with *BMPR2* mutations exhibit enhanced proliferation, altered glucose metabolism, reduced monolayer integrity, and an increased susceptibility to apoptosis.<sup>11,14–16</sup> Importantly, the silencing of *BMPR2* in human pulmonary artery endothelial cells (HPAECs) from healthy subjects reproduces many of the features of this endothelial disease phenotype.<sup>11,15,17</sup> In vivo, mice lacking *Bmpr2* in their pulmonary endothelium exhibit reduced pulmonary endothelial barrier function and have been reported to develop pulmonary hypertension spontaneously.<sup>18,19</sup>

Recently, the therapeutic administration of recombinant BMP9 was presented as a mechanism to enhance endothelial BMP signaling in PAH.<sup>11</sup> In this work, recombinant BMP9 was shown to selectively target the endothelium but not the smooth muscle cells of the pulmonary arteries. BMP9 improved monolayer integrity and blocked apoptosis, while reversing established pulmonary hypertension in both genetic and nongenetic rodent models of disease. Beyond these beneficial effects, multiple studies have also demonstrated the capacity of BMP9 to suppress VEGF (vascular endothelial growth factor) and FGF (fibroblast growth factor)-induced endothelial proliferation in

## Highlights

- *BMPR2* loss shifts the endothelial BMP (bone morphogenetic protein) 9 response from growth suppression to enhanced proliferation.
- BMP9-induced proliferation with *BMPR2* loss is linked to the prolonged induction of the canonical BMP target *ID1*.
- A  $>50\%$  reduction in *BMPR2* is required to shift the BMP9 response toward excessive proliferation.
- In vivo administration of recombinant BMP9 causes endothelial overgrowth in the retinas and lungs of endothelial-conditional *Bmpr2* knockout mice.

vitro and block angiogenesis in vivo.<sup>11,20,21</sup> However, these effects on endothelial proliferation appear to be highly context dependent, as additional studies using models of tumor vascularization or mouse embryonic stem cell-derived ECs have reported a proangiogenic role for BMP9<sup>22, 23</sup> that is mediated via a synergistic activity with TGF $\beta$  (transforming growth factor- $\beta$ ).<sup>24,25</sup> This discord regarding the pro- and antiangiogenic actions of BMP9 is particularly relevant in PAH, which is strongly associated with excessive TGF $\beta$  signaling and exhibits many features of cancer.<sup>15,26</sup> Moreover, a recent study used BMP9 knockout mice, BMP9 neutralizing antibodies, and an Alk1 (activin receptor-like kinase 1)-Fc ligand trap to demonstrate that the inhibition of endogenous BMP9 can attenuate disease severity in many of the same rodent models of PAH that were shown to benefit from administration of a recombinant form of the ligand.<sup>27</sup> Despite this uncertainty regarding the role for BMP9 in either the pathogenesis or treatment of PAH, its impact on endothelial proliferation has yet to be determined in cells from patients with PAH.

In the current study, we identify BMP9 as an angiogenic switch that can either promote or prevent endothelial proliferation, based on the level of BMPR-II expression. We also demonstrate prolonged induction of canonical BMP signaling in *BMPR2*-silenced endothelial cells, providing a mechanism by which BMP9 can drive enhanced endothelial proliferation in the context of *BMPR2* loss. These findings are potentially relevant to pathological vascular remodeling in both PAH and cancer. With the proposed translation of BMP9 as a therapy for PAH, this work may also offer a mechanism to determine which patients might benefit from BMP9-based treatments.

## MATERIALS AND METHODS

The data that support the findings of this study are available from the corresponding author upon reasonable request.

### Human Cell Culture

Blood outgrowth endothelial cells (BOECs) were generated from donor peripheral blood samples as described previously<sup>28</sup> and were confirmed for an endothelial phenotype by

flow cytometry. For BOEC generation, all blood donors provided informed consent in accordance with study 07/H0306/134 (Cambridgeshire 3 Research Ethics Committee, Cambridge, United Kingdom) or study DBMS-047-15 (Queen's University Health Sciences and Affiliated Hospitals Research Ethics Board, Kingston, Canada). BOEC lines were cultured in endothelial growth media (EGM)-2MV (Lonza, Basel, Switzerland) with 10% Premium Grade fetal bovine serum (FBS; Wisent, Saint-Jean-Baptiste, Canada) and were used for experiments between passages 4 and 8. All cell lines were confirmed to be free of mycoplasma infection. Information on the demographics and *BMPR2* mutation status of BOEC donors is detailed in Table I in the [Data Supplement](#). Unless specified otherwise, experiments involving BOEC stimulation with BMP9 were performed in EGM-2MV with 10% FBS after a 4-hour quiescence period in endothelial basal media-2 supplemented with penicillin (1 unit/mL), streptomycin (100  $\mu$ L/mL), and 2% FBS. HPAECs were purchased from Lonza and cultured in EGM-2 with 2% FBS (Lonza), as per the supplier's instructions. As with BOECs, HPAECs were quiesced in endothelial basal media-2 with 2% FBS for 4 hours before BMP9 treatment.

### siRNA Silencing

HPAECs were plated at a density of 10 500 cells/cm<sup>2</sup> and were allowed to adhere overnight. Before transfection, cells were cultured for 3 hours in Opti-MEM (ThermoFisher, Waltham, MA). Silencing of *BMPR2* was achieved using SMARTpool siRNAs (Dharmacon, Lafayette, CO) in combination with DharmaFECT 1 transfection reagent at a final siRNA concentration of 10 nmol/L, as per manufacturer's instructions. Cells were incubated in Opti-MEM with siRNA for 4 hours before being returned to culture in EGM-2 with 2% FBS. For studies examining the combined silencing of *ID1* and *BMPR2*, siRNAs were used at concentrations of 20 nmol/L and 10 nmol/L, respectively. Nontargeting control siRNAs were used as needed to top up the total siRNA concentration to 30 nmol/L. For dual silencing studies, HPAECs were cultured in EGM-2 with 5% FBS to ensure postsilencing viability.

### Proliferation Assay

BOECs, HPAECs, or mouse pulmonary endothelial cells (MPECs) were plated at 20 000 cells per well in a 24-well tissue culture plate and were left to adhere overnight. HPAECs were subjected to one extra day in culture to perform the siRNA knockdown. Cells were then quiesced for 4 hours in endothelial basal media-2 with 2% FBS before culture in full growth media (Lonza) for 96 hours, with or without 1 ng/mL human BMP9 (R&D Systems, Minneapolis, MN)—the dose used in previous studies examining the impact of BMP9 on endothelial cell function.<sup>11</sup> Media, with or without BMP9, was replenished at 48 hours after the initiation of BMP9 treatment. Proliferation of BOECs, HPAECs, and MPECs was determined by total cell count at 96 hours. Cells were trypsinized in PBS containing 2 $\times$  trypsin (20 mmol/L) and were counted by hemocytometer using trypan blue as a viability marker.

### Immunoblotting

Cells were plated in 6-cm dishes and were treated with BMP9, as described for the proliferation assay above. At 2, 24, or 72

hours post-stimulation, cells were washed once with PBS and lysed in radioimmunoprecipitation assay buffer (0.5M Tris-HCl, pH 8.0, 0.1% SDS, 1% Igepal-CA-630; all Sigma Aldrich, St. Louis, MO) containing 150 mmol/L NaCl, 10 mmol/L NaF, 0.5% sodium deoxycholate, 2 mmol/L sodium orthovanadate, and 1 $\times$  EDTA-free protease inhibitor cocktail (cComplete Mini; Roche Diagnostics, GmbH, Mannheim, Germany). Lysates were sonicated, and total protein content was quantified using the DC protein assay (Bio-Rad, Hercules, CA), as per the manufacturer's instructions. Cell lysates (8–20  $\mu$ g/well) were separated on 12% SDS-PAGE gels and transferred to polyvinylidene fluoride membranes (Millipore, Burlington, MA). The membranes were blocked with 5% nonfat milk in Tris buffered saline containing 0.05% Tween 20. Blots were probed with primary and secondary antibodies, as detailed in the [Data Supplement](#). Densitometry was performed using Bio-Rad Image Lab software.

### Apoptosis Assay

HPAECs were cultured for 72 hours in full growth media, with or without BMP9 stimulation. As detailed above, media was replaced at 48 hours of culture. Cells were then trypsinized (10 mmol/L trypsin), stained with FITC-conjugated annexin-V and propidium iodide (both BioLegend), as per the manufacturer's instructions, and assessed by flow cytometry. Apoptotic cells were defined as positive for annexin-V and negative for propidium iodide, while necrotic cells were positive for both markers.

### Metabolism Assay

HPAECs were plated at 30 000 cells per well and allowed to adhere overnight before siRNA-mediated silencing of *BMPR2*, as detailed above. The following day, cells were quiesced for 4 hours and treated for 24 hours with BMP9 before the assessment of metabolic activity. Oxygen consumption rate (OCR) and extracellular acidification rate (ECAR) were measured as markers of mitochondrial and glycolytic flux using the Seahorse XFe24 Extracellular Flux Analyzer (Agilent, North Billerica, MA). All assays were performed as described previously,<sup>29</sup> with the exception that 1 ng/mL BMP9 was added to the assay media when indicated. All data represent the average of 5 wells per condition minus the background reading.

### RNA Isolation and qPCR

RNA was harvested from cultured cells at 4, 24, or 48 hours after BMP9 stimulus or from neonatal mouse lungs at the time of sacrifice. RNA was isolated using Trizol and purified using Direct-Zol RNA isolation columns with DNase treatment (Zymo Research, Irvine, CA). Total RNA was reverse transcribed using SuperScript IV VIL0 cDNA synthesis kit (ThermoFisher), and quantitative polymerase chain reactions were performed in triplicate using PowerUp SYBR Green Master Mix (Applied Biosystems, Foster City, CA). Primer sequences are listed in Table II in the [Data Supplement](#). All primers were confirmed to have efficiencies of >90%. Relative mRNA expression was quantified relative to the appropriate reference gene using the  $\Delta\Delta$ CT method.<sup>30</sup>

### Mouse Model

Animal work was approved by the Queen's University Animal Care Committee (Kingston, Canada). Mice bearing the *L1-Cre*

construct, which expresses Cre recombinase under control of a portion of the *Alk1* promoter,<sup>31</sup> were crossed with mice possessing a floxed copy of the *Bmpr2* allele.<sup>32</sup> Offspring from this breeding were then crossed with mice bearing the *Ai6* floxed reporter construct within the *Rosa26* locus,<sup>33</sup> allowing for the conditional expression of ZsGreen (zoanthus sp. green) fluorescent protein and the recombination of floxed *Bmpr2* alleles, exclusively in cells expressing Cre recombinase (Figure 1 in the [Data Supplement](#)). All mice were from a C57BL/6J background. Male and female mice with the following genotypes were used for experimental studies: *L1-Cre<sup>+/+</sup>/Ai6<sup>+/+</sup>/Bmpr2<sup>+/+</sup>* (*Bmpr2<sup>EC+/+</sup>*), *L1-Cre<sup>+/+</sup>/Ai6<sup>+/+</sup>/Bmpr2<sup>fllox</sup>* (*Bmpr2<sup>EC+/+</sup>*), or *L1-Cre<sup>+/+</sup>/Ai6<sup>+/+</sup>/Bmpr2<sup>fllox/fllox</sup>* (*Bmpr2<sup>EC-/-</sup>*).

Mice were assigned to groups by animal identification number, allowing for the blinding of all procedures to both animal genotype and treatment until after the completion of data acquisition and analysis. No animals were excluded from analysis.

### MPEC Isolation and Culture

MPECs were isolated from 3-week-old male and female *Bmpr2<sup>EC+/+</sup>*, *Bmpr2<sup>EC+/-</sup>*, and *Bmpr2<sup>EC-/-</sup>* mice. As sex was not documented at the time of isolation, results for both sexes were analyzed together. Briefly, lungs were flushed with heparinized PBS, harvested, and digested in PBS containing 1 mg/mL collagenase/dispase and 30 µg/mL DNase (both Roche) for 45 minutes at 37 °C. Digested lungs were strained through a 40-µm filter and resuspended at 10<sup>7</sup> cells/mL in PBS with 0.5% BSA and 2 mmol/L EDTA. Cells were incubated with 25 µL/10<sup>7</sup> cells of Dynabeads (ThermoFisher), pre-conjugated to a biotinylated α-CD31 antibody (clone: MEC13.3; Biolegend, San Diego, CA) according to the manufacturer's protocol before magnetic enrichment of CD31-positive cells. Enriched cells were resuspended in EGM-2MV and plated in an uncoated T-75 for 1 hour to remove potentially contaminating fibroblasts. Nonadherent cells were collected, plated in EGM-2MV with 10% FBS at 4000 to 5000 cells per well in a collagen-coated 6-well plate, and were allowed to reach confluency. Magnetic isolation was repeated, and cells were again allowed to reach confluency before flow sorting for ZsGreen expression. MPECs were then cultured in EGM-2MV with 10% FBS and used for experiments between passages 1 and 4.

### Retinal Outgrowth and Vascular Density

Male and female *Bmpr2<sup>EC+/+</sup>*, *Bmpr2<sup>EC+/-</sup>*, and *Bmpr2<sup>EC-/-</sup>* mice were given daily intra-peritoneal (IP) injections from P2 to P6 with either 5 ng/mouse per day of carrier free human BMP9 (R&D Systems) or PBS control. Mice were euthanized at P7 by decapitation, and retinas were harvested and fixed overnight in 4% paraformaldehyde (PFA) at 4 °C. Fixed retinas were washed 3× in PBS, put into cold methanol overnight at -20 °C, washed 3× in PBS, and mounted on glass slides. Outgrowth distance from the optic disk to the vascular front was measured using a Matlab script courtesy of Josh Moskowitz (Queen's University, Center for Neuroscience). Vessel density at the vascular front was measured using the angiogenesis analyzer<sup>34</sup> plugin in ImageJ (developed at the US National Institutes of Health and available at <http://rsb.info.nih.gov/nih-image/>). Mouse genotype was determined after the completion of analysis using a tissue sample collected at the time of sacrifice. As mice were

euthanized before the age at which sex could be determined, results for both sexes were analyzed together.

### Retinal Sprouting

Retinas from P5 mouse pups were isolated and embedded in collagen (Corning) at a final concentration of 2 mg/mL with or without 1 ng/mL BMP9. For each mouse, paired retinas were imbedded with or without BMP9 treatment. After 4 hours of treatment, retinas were fixed overnight in 4% PFA, followed by dissection from the collagen, mounting, and imaging. For the quantification of sprouting, the number of tip cells migrating from the vascular front were counted for every nonoverlapping image as a measure of tip cells per field of view.

### Mouse Lung Imaging

Lungs from P7 neonatal mice treated with PBS or BMP9 were perfused with heparinized PBS before harvest and inflation via the trachea with 0.75% Phytigel (Sigma Aldrich). Lungs were then fixed overnight at 4 °C in 4% PFA and dehydrated by sequential overnight incubations in 50% ethanol at pH 9, 70% ethanol at pH 9, and 2 nights at 100% ethanol, respectively. Following dehydration, tissues were incubated overnight in ethyl cinnamate (Sigma Aldrich) for clarification before imaging on a Leica SP8 2-photon microscope.

### Statistical Analysis

Student *t* tests were used for comparisons between 2 groups. Multiple comparisons were assessed by 1- or 2-way ANOVA, followed by the appropriate post hoc test for significance, as specified in the figure legends. Equivalence of variance between experimental groups was confirmed using an *F* test for comparisons between 2 groups and a Brown-Forsythe test in conjunction with ANOVA, when applicable. Normal distribution was assumed for all statistical analyses, with the exception of the comparison of BMP9-induced proliferative effects in BOECs from PAH patients and control subjects. For this case, a nonparametric Mann-Whitney *U* test was used. All statistical tests used 2-sided tests of significance. All data are reported as mean±SEM. The use of small sample sizes (eg, n=3) was limited to technical replicates within the same cell line.

## RESULTS

### BMP9 Promotes Endothelial Cell Proliferation in the Absence of *BMPR2*

In agreement with previous reports examining the effect of BMP9 on HPAECs,<sup>11,35</sup> BMP9 treatment at 1 ng/mL suppressed the proliferation of BOECs from both healthy control subjects and PAH patients lacking *BMPR2* mutations (Figure 1A; Table I in the [Data Supplement](#)). In marked contrast, BOECs from PAH patients with *BMPR2* mutations exhibited significantly increased proliferation in response to BMP9. Immunoblotting for BMPR-II protein (Figure 1B) demonstrated a negative correlation between BMPR-II receptor levels and the proliferative response to BMP9, with the PAH patient cell lines displaying

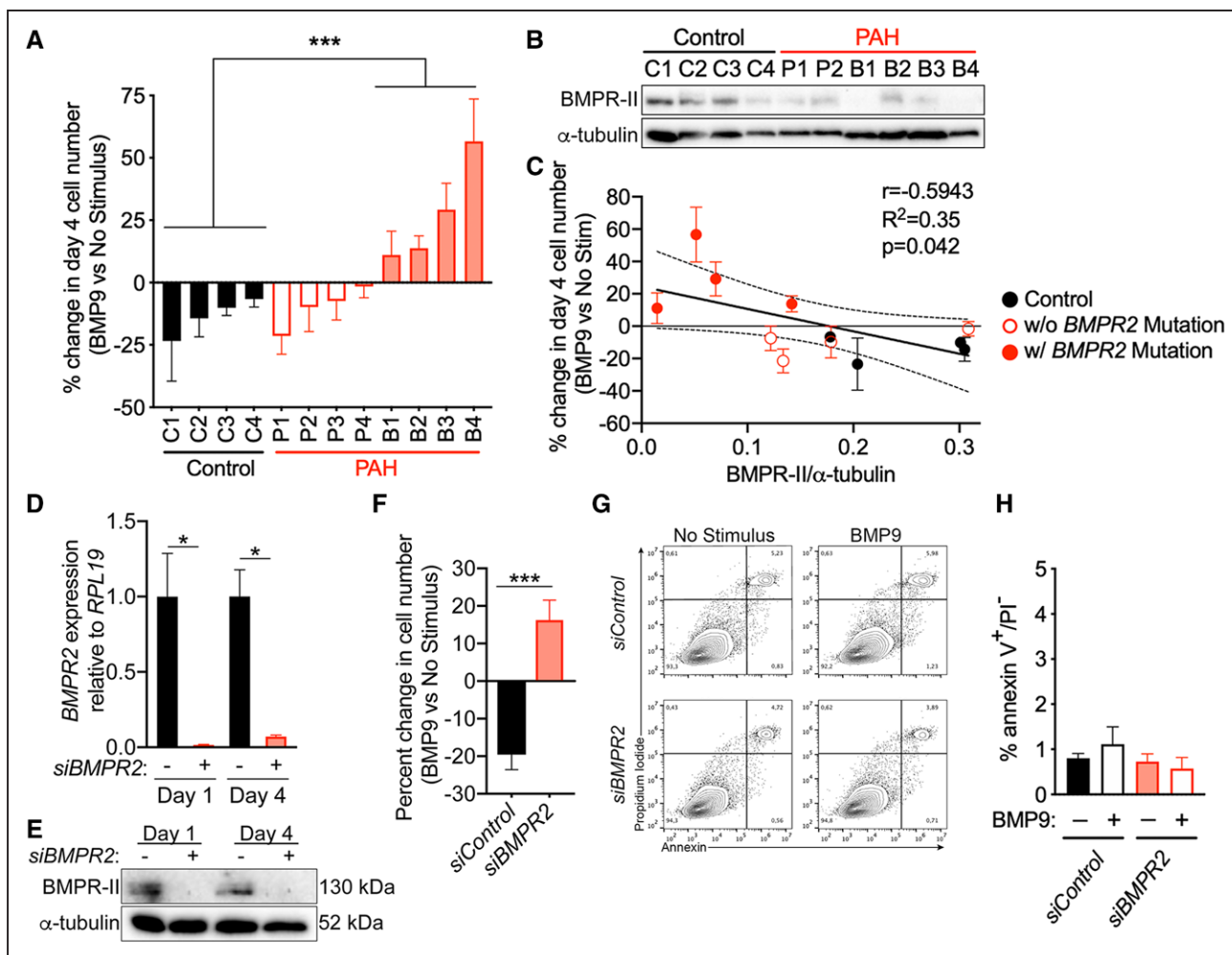


**Figure 1. BMPR2 loss causes BMP (bone morphogenetic protein) 9–induced cell proliferation.**

**A**, Analysis of percentage change in BOEC number after 4 d of culture with or without BMP9 (1 ng/mL). BOEC lines include healthy controls (C1–4, black), pulmonary arterial hypertension (PAH) patients with *BMPR2* mutations (B1–4, solid red), and PAH patients without *BMPR2* mutations (P1–4, red outline) ( $n=3–8$  repeats per cell line). **B**, Immunoblot of BMPR-II (BMP receptor 2) levels in BOEC lines relative to  $\alpha$ -tubulin as a loading control. **C**, Linear regression plot between the BOEC proliferative response to BMP9 and BMPR-II protein expression, normalized to  $\alpha$ -tubulin levels.  $R^2$  and  $P$  are indicated on the graph. **D**, Validation of *siBMPR2* knockdown at 1 and 4 d post-siRNA transfection by quantitative polymerase chain reaction. *BMPR2* expression levels are shown relative to *RPL19* ( $n=3$ ). **E**, Representative immunoblot of HPAEC BMPR-II levels with or without siRNA silencing of *BMPR2* at 1 and 4 d after siRNA treatment, with or without BMP9 stimulus. **F**, Analysis of percentage change in control and *BMPR2*-silenced HPAEC number after 4 d of culture with or without BMP9 (1 ng/mL) ( $n=5$ ). **G**, Representative flow cytometry plots of annexin-V and propidium iodide (PI) staining in control and *BMPR2*-silenced HPAECs after 72 h of culture with or without BMP9 (1 ng/mL). **H**, Quantification of apoptotic HPAECs (annexin-V<sup>+</sup>/PI<sup>-</sup>) as a percentage of total cells ( $n=3$ ). Control and mutation bearing BOEC lines in **A** were compared using a Mann-Whitney  $U$  test. Unpaired Student  $t$  tests were used in **D** and **F**. One-way ANOVA, with a Tukey post hoc test was used in **H**. A sample  $t$  test against the theoretical mean of zero was used in **F**. Error bars are mean $\pm$ SEM. \* $P<0.05$ , \*\* $P<0.01$ , \*\*\* $P<0.001$ ; # $P<0.05$ , ## $P<0.01$ .

pronounced reductions in BMPR-II also exhibiting the greatest proliferative response to BMP9 treatment (Figure 1C). A similar correlation was observed between BMP9-induced proliferation and *BMPR2* gene expression (Figure II in the Data Supplement), with a significant reduction in *BMPR2* levels being observed exclusively in the subset of PAH patients bearing *BMPR2* mutations.

To test the possibility that *BMPR2* loss was driving BMP9-induced proliferation in patient BOECs, we examined the BMP9 response in HPAECs following siRNA-mediated *BMPR2* knockdown. SiRNA *BMPR2* silencing caused a >95% reduction in *BMPR2* gene and protein

expression that persisted from 1 to 4 days post-siRNA knockdown, corresponding to the first 72 hours of BMP9 treatment (Figure 1D and 1E). While BMP9 significantly reduced the proliferation of HPAECs transfected with nontargeting control siRNA, silencing of *BMPR2* in these cells recapitulated the proliferative response to BMP9 that was observed in BOECs from *BMPR2* mutation bearing PAH patients (Figure 1F). To confirm that these changes in cell number were not the consequence of altered levels of apoptotic cell death, apoptosis was measured by the flow cytometric analysis of annexin-V/propidium iodide on HPAECs (Figure 1G). Basal apoptosis

was extremely low under these conditions ( $\approx 1\%$ ), with no differences observed between groups in response to *BMPR2* silencing or BMP9 treatment (Figure 1H). Assessment of necrotic cells, largely resulting as a consequence of trypsinization before analysis, also revealed no differences between groups (Figure III in the [Data Supplement](#)).

### BMP9-Induced Endothelial Proliferation Is Not Due to Changes in Glycolytic or Oxidative Metabolism

Previous reports have indicated that endothelial cells from PAH patients exhibit uncoupled aerobic glycolysis and that silencing *BMPR2* is sufficient to increase glycolytic activity in control HPAECs.<sup>15,16</sup> To determine whether altered metabolism was responsible for driving BMP9-induced proliferation in *BMPR2*-silenced HPAECs, the metabolic response of these cells to BMP9 was quantified by Seahorse analyzer. For this assay, OCR and ECAR were used as measures of oxidative and glycolytic metabolism, respectively. BMP9 treatment caused a coupled reduction of both OCR and ECAR in control HPAECs relative to their untreated control (Figure 2A through 2D), which was in keeping with the antiproliferative effect of BMP9 in these cells. In contrast to previous studies showing elevated glycolysis in *BMPR2*-silenced HPAECs,<sup>15,16</sup> *BMPR2* knockdown did not increase OCR or ECAR and was actually found to decrease baseline glycolytic metabolism in these cells (Figure 2B and 2D). Silencing of *BMPR2* also eliminated the BMP9-induced reduction of both oxidative and glycolytic metabolism that was observed in siRNA control-treated HPAECs. Importantly, neither *BMPR2* silencing nor BMP9 treatment caused a significant difference in the ratio of OCR to ECAR (Figure 2E), indicating that BMP9-induced proliferation in *BMPR2*-deficient endothelial cells is not a consequence of an uncoupling of glycolysis from oxidative metabolism.

### *BMPR2* Loss Alters the Kinetics of BMP9-Mediated *Id* Induction

The transcriptional regulators, *ID1* and *ID2*, are downstream targets of canonical BMP signaling that promote cell proliferation.<sup>36</sup> Examination of *ID* gene expression showed that both *ID1* and *ID2* were induced as early as 4 hours after the initiation of BMP9 treatment in the siRNA control-treated HPAECs, relative to their respective untreated controls (Figure 3A and 3B). While this induction returned to baseline by 24 hours post-stimulus in control HPAECs, *BMPR2*-silenced HPAECs exhibited a prolonged induction of both *ID1* and *ID2* that was delayed until 24 hours after the initiation of BMP9 treatment and only returned to baseline levels at the 48-hour time point. This sustained *ID* induction

was confirmed by immunoblotting for *Id1* protein, which was increased exclusively in *BMPR2*-silenced HPAECs at 24 hours after the initiation of BMP9 treatment (Figure 3C and 3D).

An assessment of upstream canonical signaling identified a similar delay in the kinetics of Smad1/5/9 phosphorylation with *BMPR2* knockdown. While control HPAECs exhibited an increase in Smad1/5/9 phosphorylation after 2 hours of BMP9 exposure that returned to baseline by 24 hours, *BMPR2*-silenced cells exhibited no acute response to BMP9 and were instead found to upregulate Smad1/5/9 phosphorylation only after 24 hours of BMP9 treatment, in line with increased *Id1* expression at this time point (Figure 3C and 3E). Examination of total Smad1 identified a significant reduction in protein levels in HPAECs following chronic BMP9 stimulation (Figure 3C and 3F). Although this reduction was only observed in control HPAECs after 72 hours of BMP9 treatment, it was more pronounced in the *BMPR2*-silenced HPAECs, which displayed a BMP9-induced reduction in total Smad1 protein across all experimental time points. When taking this change in total Smad1 levels into account, the quantification of phosphorylated Smad1/5/9 as a proportion of total available Smad1 highlighted the prolonged activation of canonical BMP signaling in BMP9-treated, *BMPR2*-silenced HPAECs (Figure 3G). Interestingly, this activation appeared to persist as far out as 72 hours after the initiation of treatment, although not at a level that was significantly different from its respective untreated control. This combination of increased phosphorylation and decreased total Smad levels with BMP9 treatment is indicative of chronic activation of canonical signaling in *BMPR2*-silenced HPAECs.<sup>37</sup>

While our findings point to *BMPR2* loss as the primary factor driving BMP9-induced endothelial cell proliferation, previous studies reporting a role for BMP9 in the promotion of angiogenesis have attributed this effect to a synergistic enhancement of proangiogenic TGF $\beta$  signaling. An examination of both Smad2/3 and Smad1/5/9 phosphorylation identified no such synergistic effects between BMP9 and TGF $\beta$  in HPAECs, with or without *BMPR2* silencing (Figure IV in the [Data Supplement](#)). To confirm the importance of altered canonical signaling kinetics and prolonged *ID* induction to BMP9-induced proliferation in the absence of *BMPR2*, *ID1* was silenced, either alone or in combination with *BMPR2* knockdown (Figure 3H and 3I). While *ID1* silencing alone had no impact on BMP9-induced growth suppression in HPAECs, the dual silencing of both *ID1* and *BMPR2* resulted in a significant blunting of BMP9-induced proliferation, when compared with cells treated with siRNA targeting *BMPR2* alone (Figure 3J).

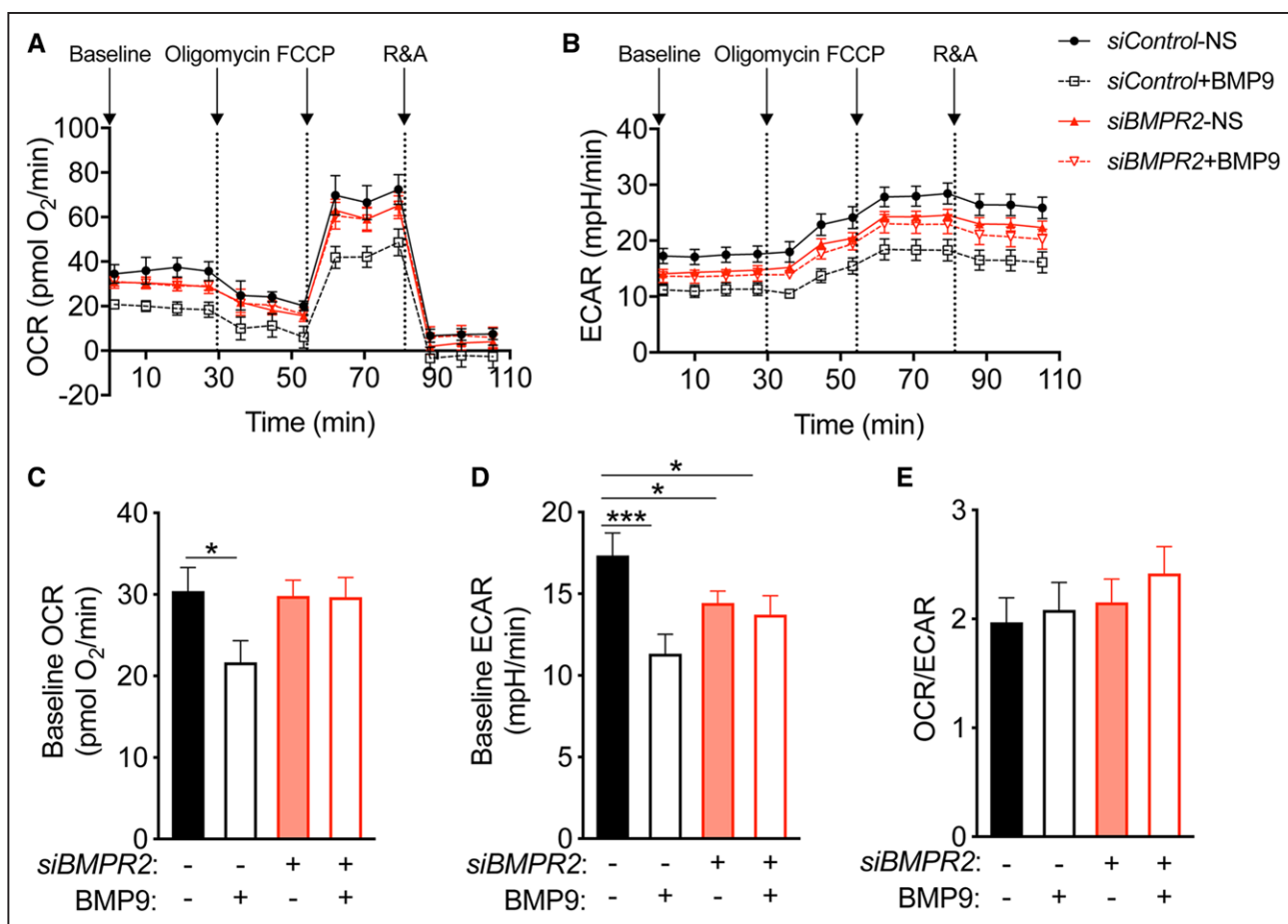


**Figure 2. BMP2 loss prevents the reduction of glycolytic and oxidative metabolism by BMP (bone morphogenetic protein) 9.** Control and *BMPR2*-silenced HPAECs were cultured for 24 h with or without BMP9 (1 ng/mL) before analysis on a Seahorse XFe24 Extracellular Flux Analyzer. Oxygen consumption rate (OCR; **A**) and extracellular acidification rate (ECAR; **B**) were measured as markers of mitochondrial and glycolytic flux. In both **A** and **B**, oligomycin was added to measure ATP production, while carbonyl cyanide-4 (trifluoromethoxy) phenylhydrazine (FCCP) was added to uncouple oxygen production from ATP production and measure maximal oxygen consumption. Rotenone and antimycin A (R&A) inhibit complex I and complex III, respectively, to shut down oxidative metabolism. **C**, Quantification of baseline OCR measurements. **D**, Quantification of baseline ECAR measurements. **E**, Analysis of coupled oxidative and glycolytic metabolism, processed by measurement of baseline OCR/ECAR ratio.  $n=3$ , 5 wells/condition. Unpaired *t* test between groups. Bars are mean $\pm$ SEM. ns indicates nonsignificant. \* $P<0.05$ , \*\*\* $P<0.001$ .

### BMP9-Induced Endothelial Proliferation Requires *Bmpr2* Sub-Haploinsufficiency

Although PAH is associated with heterozygous germline mutations in *BMPR2*, a significant proportion of PAH patients, with or without *BMPR2* mutations, exhibit a near-complete loss of BMPR-II protein in their endothelium.<sup>9</sup> To determine whether this BMPR-II sub-haploinsufficiency is required to induce a proliferative response to BMP9, conditional knockout mice that were either WT (wild type; *Bmpr2*<sup>EC+/+</sup>), heterozygous (*Bmpr2*<sup>EC+/-</sup>), or homozygous null (*Bmpr2*<sup>EC-/-</sup>) for *Bmpr2* in their pulmonary endothelium were created by crossing mice bearing the floxed *Bmpr2* allele<sup>32</sup> with mice expressing Cre recombinase under control of the *L1* promoter.<sup>31</sup> These animals were also crossed with mice harboring the *Ai6* Cre-driven reporter construct,<sup>33</sup> resulting in the expression of the ZsGreen fluorescent protein in the

Cre<sup>+</sup> cells of the pulmonary vascular endothelium (Figure I in the [Data Supplement](#)).

Magnetic sorting of CD31<sup>+</sup> cells from the lungs of *Bmpr2*<sup>EC+/+</sup>, *Bmpr2*<sup>EC+/-</sup>, or *Bmpr2*<sup>EC-/-</sup> mice produced populations of cells that were uniformly CD31<sup>+</sup> (Figure 4A), but included both ZsGreen<sup>+</sup> MPECs and a ZsGreen<sup>-</sup> subset that likely consisted of contaminating CD31<sup>+</sup> lymphatic endothelial cells (Figure 4B). Flow sorting for ZsGreen<sup>+</sup> cells produced a uniform CD31<sup>+</sup>ZsGreen<sup>+</sup> MPEC population (Figure 4B and 4C). The homozygous or heterozygous deletion of *Bmpr2* in these cells was confirmed by immunoblotting for BMPR-II protein, which showed either a partial or complete loss of BMPR-II in MPECs from *Bmpr2*<sup>EC+/-</sup> and *Bmpr2*<sup>EC-/-</sup> mice, respectively (Figure 4D). As in control HPAECs and BOECs from healthy subjects, BMP9 significantly reduced proliferation in MPECs from *Bmpr2*<sup>EC+/+</sup> mice (Figure 4E). In contrast, MPECs from *Bmpr2*<sup>EC+/-</sup> mice

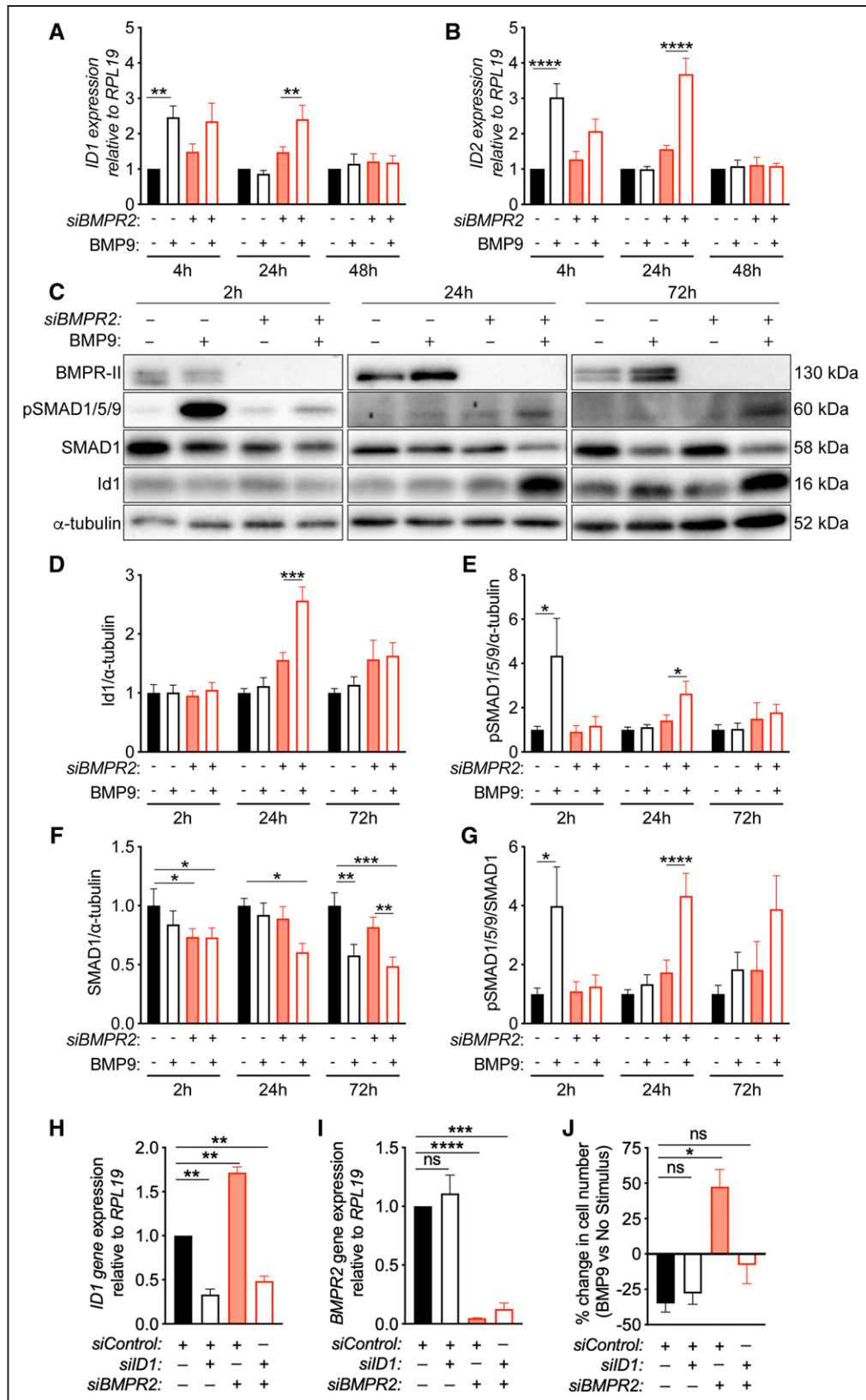


**Figure 3. BMPR2 loss alters the kinetics of BMP (bone morphogenetic protein) 9–mediated Id (inhibitor of DNA binding/ inhibitor of differentiation) induction.**

Analysis of (A) *ID1* and (B) *ID2* as canonical downstream gene targets of BMP9 signaling in control and *BMPR2*-silenced HPAECs, with or without BMP9 (1 ng/mL) treatment for 4 (n=10), 24 (n=7), or 48 (n=3) h. Values of *ID* gene expression relative to *RPL19* are expressed as the fold change normalized to *siControl* HPAECs without stimulus. C, Representative immunoblots for BMPR-II (BMP receptor 2), (Continued)



exhibited no significant response to BMP9, whereas the proliferation of MPECs from *Bmpr2<sup>EC-/-</sup>* mice was significantly increased in response to BMP9 exposure. These findings are consistent with a gene dosing effect of *Bmpr2* loss on the endothelial BMP9 response and indicate that a >50% reduction of *Bmpr2* is required for BMP9 to induce endothelial proliferation.

### Endothelial Deletion of *Bmpr2* Causes BMP9-Induced Angiogenesis In Vivo

While initial reports characterizing the pattern of Cre expression in *L1-Cre* mice suggested that Cre-mediated recombination in these mice was largely limited to the pulmonary endothelium,<sup>19,31,38</sup> these studies also demonstrated some degree of Cre-mediated recombination in other tissues, including the brain. An examination of ZsGreen expression in a variety of tissues from *Bmpr2<sup>EC+/+</sup>* mice identified Cre recombinase activity not only in the lung vasculature but also in the endothelium of the brain and retina (Figure VA through VC in the [Data Supplement](#)). A small degree of nonendothelial expression of ZsGreen was also observed in the liver, heart, and kidney (Figure VD through VF in the [Data Supplement](#)). Importantly, this identification of Cre-mediated recombination in the retinal endothelium allowed for an in vivo examination of the impact of BMP9 on neonatal retinal angiogenesis in the context of both heterozygous and homozygous *Bmpr2* deletion.

An assessment of retinal vascular network complexity in postnatal day (P) 7 pups treated IP with PBS vehicle control from P2 to P6 identified a significant impairment in baseline vascular network development in *Bmpr2<sup>EC+/-</sup>* and *Bmpr2<sup>EC-/-</sup>* mice, when compared with *Bmpr2<sup>EC+/+</sup>* controls (Figure 5A through 5C; Figure VIA and VIB in the [Data Supplement](#)). This finding, which agrees with a previous report of reduced retinal vascularization with *Bmpr2* loss,<sup>39</sup> was supported by in vitro matrigel assays that demonstrated a significant decrease in network complexity in *BMPR2*-silenced HPAECs (Figure VIC and VID in the [Data Supplement](#)). In addition to these baseline differences, in vivo administration of BMP9 from P2 to P6 (5 ng/mouse per day, IP) was found to reduce vascular network complexity in the retinas of *Bmpr2<sup>EC+/+</sup>* mice (Figure 5B and 5C). In contrast, this dose of BMP9, which is generally equivalent on a nanogram/kilogram basis to the dose used in previous animal

studies,<sup>11</sup> had no effect on the retinal vasculature of *Bmpr2<sup>EC+/-</sup>* animals and significantly increased vascular density in retinas from *Bmpr2<sup>EC-/-</sup>* mice (Figure 5B and 5C). Interestingly, a parallel examination of retinal vascular outgrowth distance from the optic disk did not identify any impact of *Bmpr2* deletion or BMP9 treatment on this measure (Figure 5A and 5D). This finding was supported by ex vivo studies showing no impact of BMP9 treatment on tip cell formation in collagen-embedded P5 retinas, independent of endothelial *Bmpr2* genotype (Figure 5E and 5F).

In addition to the retinal vasculature, the impact of *Bmpr2* loss on the in vivo BMP9 response was also assessed in the pulmonary circulation of the mice given daily BMP9 from P2 to P6. In contrast to the retinal analysis, BMP9 administration had no measurable impact on ZsGreen levels in the lungs of *Bmpr2<sup>EC+/+</sup>* mice, despite a noticeable impact on lung morphology and the distribution of ZsGreen<sup>+</sup> cells in these animals (Figure 6A, 6D, and 6G). This result suggests that BMP9 treatment may impact endothelial cell branching and postnatal lung vascular development in WT mice without impacting overall endothelial cell number in the lungs of these animals. This altered lung morphology, which was also observed in both treated and untreated *Bmpr2<sup>EC+/-</sup>* and *Bmpr2<sup>EC-/-</sup>* mice, is in keeping with reports identifying an important role for angiogenesis in postnatal pulmonary alveolarization.<sup>40</sup> As with the retinal vasculature, BMP9 administration induced significant endothelial overgrowth in the lungs of *Bmpr2<sup>EC-/-</sup>* animals (Figure 6C, 6F, and 6G). Further examination of the impact of endothelial *Bmpr2* loss on pulmonary inflammation identified no changes in IL (interleukin)-6, TNF $\alpha$  (tumor necrosis factor alpha), or IL-1 $\beta$  gene expression in the lungs, with or without BMP9 treatment (Figure VIIA through VIIC in the [Data Supplement](#)). Similarly, PAI-1 (plasminogen activator inhibitor-1) expression was examined as a surrogate for TGF $\beta$  activity but was not impacted by BMP9 across all *Bmpr2* genotypes (Figure VIID in the [Data Supplement](#)).

## DISCUSSION

We report a *BMPR2*-dependent shift in the endothelial proliferative response to BMP9, from the suppression of proliferation in BOECs from healthy donors to enhanced proliferation in cells from *BMPR2* mutation bearing PAH patients. siRNA-mediated silencing of *BMPR2*

**Figure 3 Continued.** phosphorylated SMAD (pSMAD) 1/5/9, SMAD1, Id1, and  $\alpha$ -tubulin at 2 (n=9), 24 (n=6), and 72 (n=6) h after the initiation of BMP9 stimulus. **D–F**, Quantification of **(D)** Id1, **(E)** pSMAD1/5/9, and **(F)** total SMAD1 relative to  $\alpha$ -tubulin. **G**, Quantification of pSMAD1/5/9 relative to total SMAD1. Two-way ANOVA with Sidak multiple comparisons post hoc test was used to determine differences between the BMP9-treated group and its respective no stimulus control for the assessment of *ID* gene expression, Id1 protein, and pSMAD1/5/9 levels. Two-way ANOVA with Tukey multiple comparisons post hoc test was used to determine differences in total SMAD1 levels between all treatment groups. **H** and **I**, Validation of **(H)** *siID1* and **(I)** *siBMPR2* knockdowns in HPAECs by quantitative polymerase chain reaction. *ID1* and *BMPR2* expression levels are shown relative to *RPL19* (n=4). **J**, Analysis of percentage change in control, *ID1*-silenced, *BMPR2*-silenced, or dual-silenced HPAEC number after 4 d of culture with or without 1 ng/mL BMP9 (n=4). One-way ANOVA, with a Dunnett post hoc test. Error bars are mean $\pm$ SEM. ns indicates nonsignificant. \* $P$ <0.05, \*\* $P$ <0.01, \*\*\* $P$ <0.001, \*\*\*\* $P$ <0.0001.

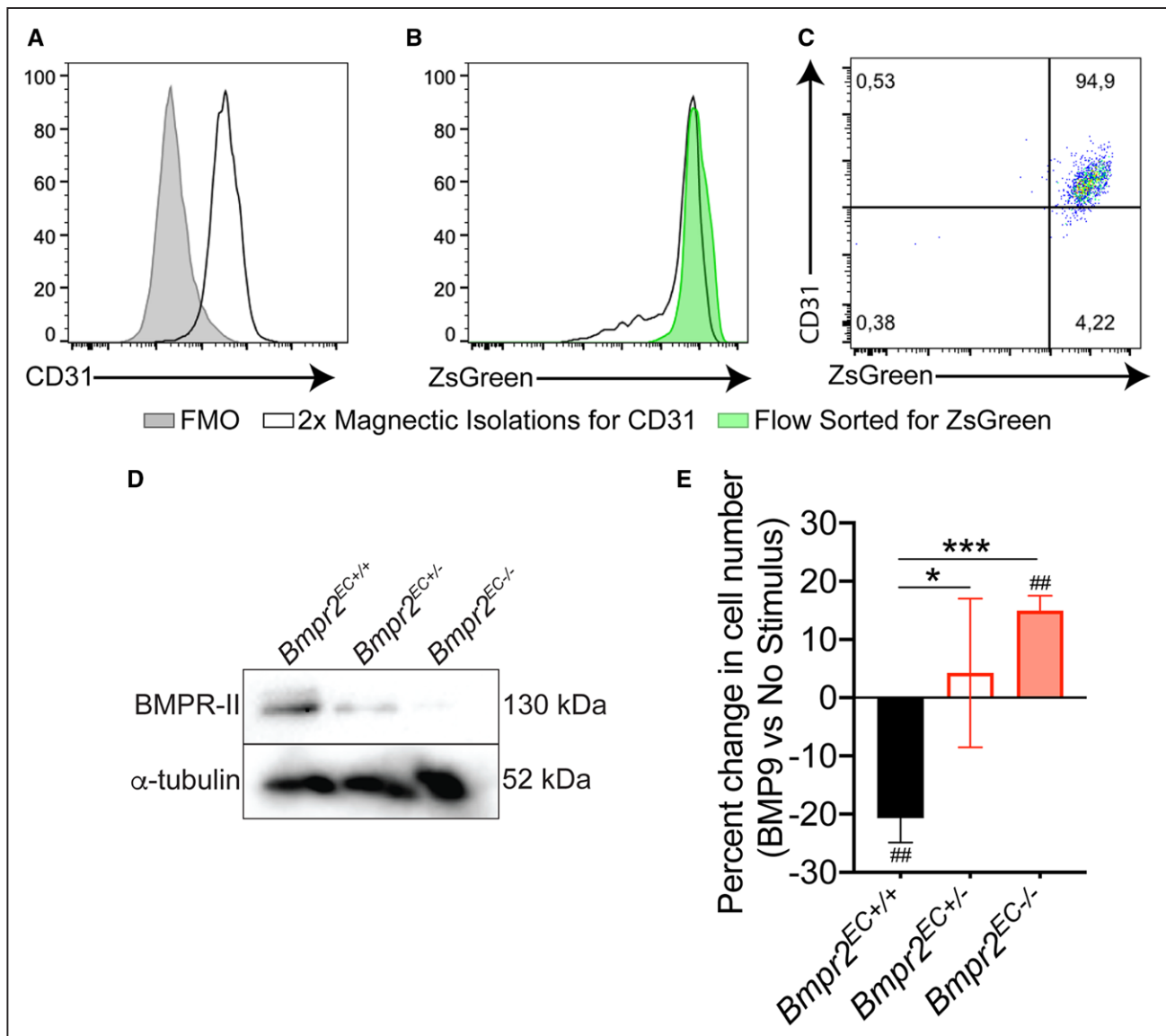


**Figure 4. Pulmonary endothelial cells from *Bmpr2*<sup>EC-/-</sup> mice proliferate in response to BMP (bone morphogenetic protein) 9.** Representative flow cytometry plots of (A) CD31 and (B) ZsGreen (zoanthus sp. green) expression by MPECs, after 2 magnetic isolations for CD31 (black line) and after being flow sorted for ZsGreen positivity (green shading). C, Flow-sorted cells were confirmed to be ZsGreen and CD31 positive. D, Representative immunoblot of BMPR-II (BMP receptor 2) protein levels in MPECs from *Bmpr2*<sup>EC+/+</sup>, *Bmpr2*<sup>EC+/-</sup>, and *Bmpr2*<sup>EC-/-</sup> mice, relative to  $\alpha$ -tubulin as a loading control. E, Analysis of percentage change in cell proliferation of isolated pulmonary endothelial cells from *Bmpr2*<sup>EC+/+</sup>, *Bmpr2*<sup>EC+/-</sup>, and *Bmpr2*<sup>EC-/-</sup> mice, cultured for 4 d with or without BMP9 (1 ng/mL). n=6, 3, and 5, respectively. One-way ANOVA, with a Tukey post hoc test was used in E. A sample *t* test against the theoretical mean of zero was used in E. Error bars are mean $\pm$ SEM. \**P*<0.05, \*\*\**P*<0.001; ##*P*<0.01. FMO indicates fluorescence minus one control.

recapitulated this cellular phenotype in control HPAECs, confirming that the effect was indeed the direct result of *BMPR2* loss and was not a secondary consequence of interindividual variability or the examination of BOECs from patients with established disease. Our assessment of the molecular mechanisms driving this shift demonstrated that *BMPR2* loss causes an alteration in the kinetics of BMP9-induced canonical signaling that is defined by delayed Smad phosphorylation and a sustained induction of both *ID* gene expression and Id1 protein levels.

Considering the well-established role for Id (inhibitor of DNA binding/inhibitor of differentiation) proteins in

promoting cell proliferation in cancer,<sup>36</sup> our identification of Id upregulation with chronic BMP9 exposure offers valuable mechanistic insight to explain how *BMPR2* loss can drive excessive proliferation in response to BMP9. Additional studies exploring the silencing of *ID1* demonstrated that this prolonged induction of canonical signaling is indeed central to BMP9-induced endothelial proliferation in the absence of *BMPR2*. It is also worth noting that BMP9 is one of the few BMPs to be found in the circulation,<sup>20</sup> where it is present at  $\approx$ 300 pg/mL, similar to the 1 ng/mL used in our in vitro studies. While previous studies examining impact of *BMPR2* loss on

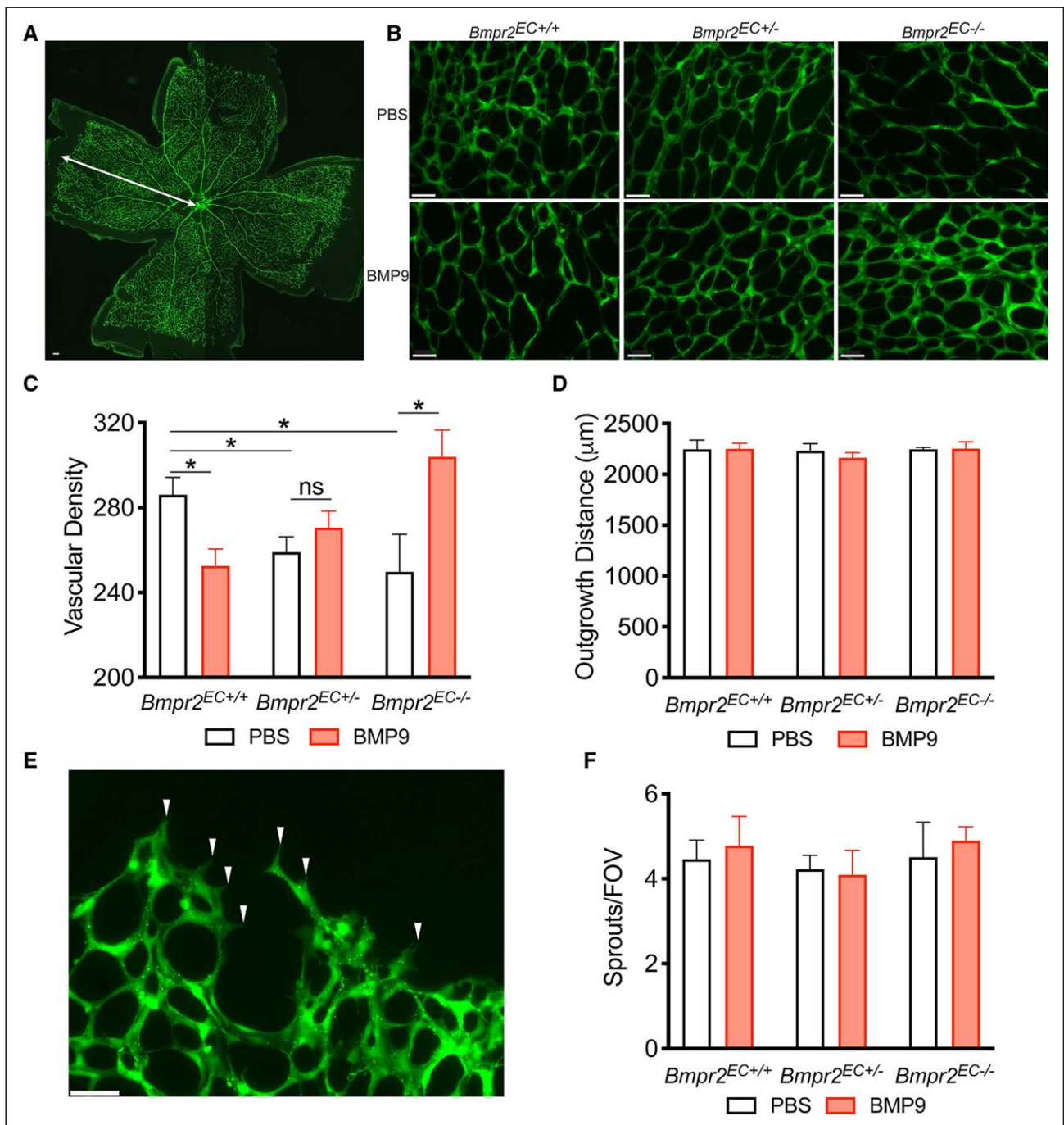


**Figure 5. Endothelial *Bmpr2* expression dictates the impact of systemic BMP (bone morphogenetic protein) 9 treatment on neonatal retinal angiogenesis.**

**A**, Representative postnatal day (P) 7 retina from a *Bmpr2*<sup>EC+/+</sup> mouse expressing ZsGreen (zoanthus sp. green) in the retinal endothelium. White arrow indicates vascular outgrowth distance from the optic disc. **B**, Representative vascular bed images from P7 *Bmpr2*<sup>EC+/+</sup>, *Bmpr2*<sup>EC+/-</sup>, and *Bmpr2*<sup>EC-/-</sup> pups following the intra-peritoneal administration of either PBS or BMP9 (5 ng/mouse per day, IP) from P2 to P6. **C**, Quantification of branching points as a measure of vascular density. *Bmpr2*<sup>EC+/+</sup>: PBS (n=12), BMP9 (n=15); *Bmpr2*<sup>EC+/-</sup>: PBS (n=23), BMP9 (n=24); *Bmpr2*<sup>EC-/-</sup>: PBS (n=6), BMP9 (n=9). Two-way ANOVA, with Sidak multiple comparisons post hoc test was used to compare between treated and untreated groups within each genotype. A Dunnett post hoc test was used to compare untreated retinas to the *Bmpr2*<sup>EC+/+</sup> control across genotypes. **D**, Quantification of vascular outgrowth from the optic disk. *Bmpr2*<sup>EC+/+</sup>: PBS (n=6), BMP9 (n=11); *Bmpr2*<sup>EC+/-</sup>: PBS (n=16), BMP9 (n=19); *Bmpr2*<sup>EC-/-</sup>: PBS (n=4), BMP9 (n=5). **E**, Representative image of the vascular front in a P5 retina following 4 h of ex vivo culture. Tip cells are indicated by white triangles. **F**, Quantification of tip cells per field of view (FOV) from P5 retinas following 4 h of ex vivo culture, with or without BMP9 (1 ng/mL). *Bmpr2*<sup>EC+/+</sup>, n=5; *Bmpr2*<sup>EC+/-</sup>, n=9; and *Bmpr2*<sup>EC-/-</sup>, n=3. Error bars are mean±SEM. ns indicates nonsignificant. \**P*<0.05. FOV indicates field of view.

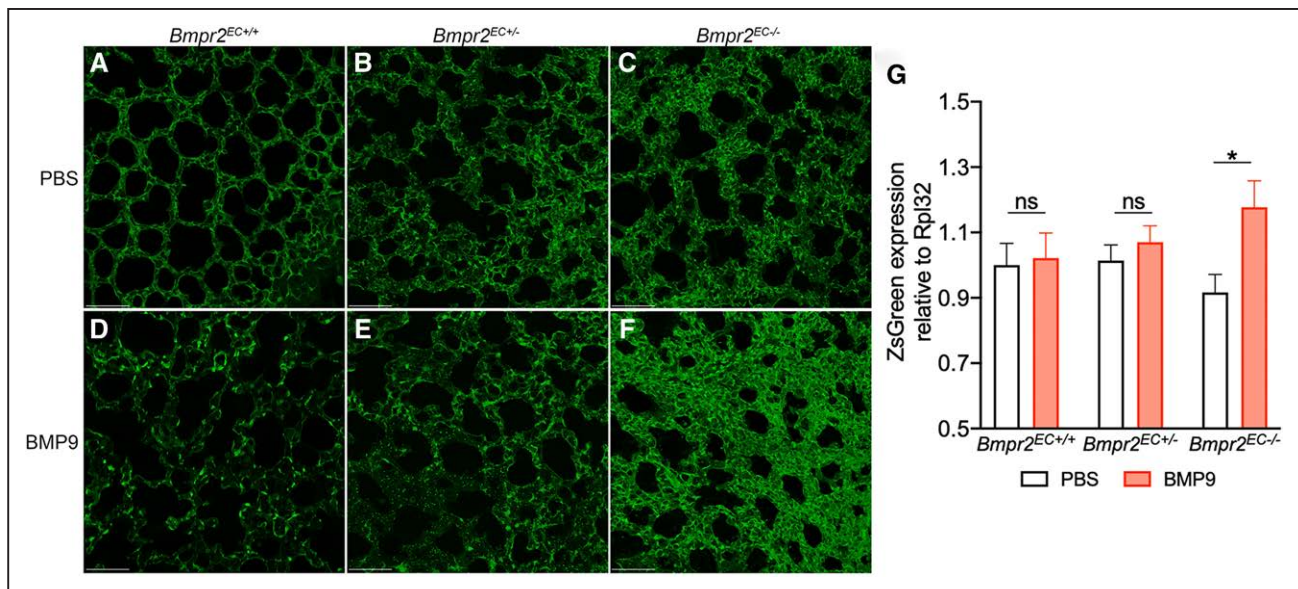


**Figure 6. BMP (bone morphogenetic protein) 9 induces hyperproliferative endothelial overgrowth in the lungs of neonatal *Bmpr2<sup>EC-/-</sup>* mice.**

*Bmpr2<sup>EC+/+</sup>* (A and D), *Bmpr2<sup>EC+/-</sup>* (B and E), and *Bmpr2<sup>EC-/-</sup>* (C and F) mouse pups were treated with (A–C) PBS or (D–F) BMP9 (5 ng/mouse per day, IP) from postnatal day (P) 2 to 6. Lungs were harvested on P7, clarified and imaged by 2-photon confocal microscopy for ZsGreen<sup>+</sup> (zoanthus sp. green) endothelial cells, which are seen in bright green above the background autofluorescence of lung tissue. Images are representative 10- $\mu$ m z stacks from pups of each genotype and treatment group. Scale bar=20  $\mu$ m. G, Quantification of lung ZsGreen expression as a measure of pulmonary endothelial cell content (n=10–23). Two-way ANOVA, with Sidak multiple comparisons post hoc test, was used to compare between treated and untreated groups within each genotype. Error bars are mean $\pm$ SEM. ns indicates nonsignificant. \* $P$ <0.05.

canonical signaling in HPAECs demonstrated either no impact of *BMPR2* silencing on BMP9-induced *ID* expression<sup>35</sup> or an impairment of *ID* induction in *BMPR2*-silenced HPAECs treated with BMP4,<sup>13</sup> these reports focused exclusively on the acute effects achieved over a few hours of BMP treatment. In contrast, our examination of canonical signaling at later time points in response to chronic BMP9 exposure takes into account the role of BMP9 as a circulating factor that is perpetually stimulating the vascular endothelium.

When taken together, the current study helps to clarify the already complex literature surrounding the contribution of BMP9 to either the promotion or prevention of angiogenesis, as well as the potential role for BMP9 signaling in both the pathogenesis of PAH and the regulation of tumor vascularization. Previous reports suggesting a proangiogenic role for BMP9 attributed this action to a synergistic enhancement of TGF $\beta$  signaling in the tumor microenvironment.<sup>24</sup> Our work failed to show any such synergy of BMP9 with canonical TGF $\beta$  signaling in the pulmonary endothelium, with or without *BMPR2* silencing. In contrast, we confirmed earlier work showing that HPAECs are minimally responsive to TGF $\beta$ <sup>35</sup> and demonstrated that *BMPR2* knockdown instead results in impaired BMP9-induced phosphorylation of Smad2—a downstream target of both TGF $\beta$  and BMP9.

It is noteworthy that our in vitro findings were validated in vivo in 2 distinct vascular beds. In both the lungs and the retina of neonatal mice, *Bmpr2* loss was shown

to negatively impact vascular structure at baseline, independent of exogenous BMP9 delivery. More importantly, our demonstration that BMP9 administration suppresses vascular network formation in *Bmpr2<sup>EC+/+</sup>* mice, while enhancing endothelial growth in *Bmpr2<sup>EC-/-</sup>* conditional knockouts, illustrates how this single factor can either promote vascular stability or drive vascular hyperproliferation in a manner that is dependent on the availability of BMPR-II. In addition to providing this in vivo validation, work in MPECs from the *Bmpr2<sup>EC+/+</sup>* and *Bmpr2<sup>EC-/-</sup>* conditional knockout mice also allowed for the identification of a gene dosing effect of *Bmpr2* loss in the endothelial BMP9 response, where a >50% reduction of *Bmpr2* expression is required to shift this response toward the stimulation of enhanced proliferation.

Critically, previous studies examining the impact of BMP9 on the pathogenesis of PAH have only examined models of partial *Bmpr2* loss, including the *Bmpr2<sup>+/-R899X</sup>* heterozygous knock-in mouse model,<sup>11</sup> or nongenetic models that are associated with reduced BMPR-II expression, such as the monocrotaline rat.<sup>41</sup> Although valuable as preclinical research tools, these models do not reproduce the near-complete BMPR-II deficiency that is observed in many patients with PAH. Future studies exploring the impact of BMP9 administration on the pathophysiology of PAH in the *Bmpr2<sup>EC-/-</sup>* conditional knockout, either at baseline or in response to PAH-inducing stimuli like chronic hypoxia or 5-lipoxygenase overexpression,<sup>42,43</sup> will help to establish the functional

relevance of our current findings to this subset of *BMPR2*-deficient PAH patients.

The concept that additional disease-associated factors, beyond *BMPR2* mutation alone, may be needed to push *BMPR2* expression below the threshold required for a proliferative response to BMP9 may help to explain the reduced penetrance of PAH in individuals bearing heterozygous germline *BMPR2* mutations. This identification of BMP9 signaling as a balance between pro- and antiangioproliferative effects, which shifts with changes in *BMPR-II* expression, can also serve to reconcile seemingly conflicting reports that BMP9 either attenuates or enhances disease severity in rodent models of PAH.<sup>27</sup> As detailed above, these rodent models offer an intermediate level of *BMPR-II* loss, in which the manipulation of BMP9 bioavailability, though the administration of recombinant protein or the blockade of the endogenous ligand, could have dramatically different effects, depending on the balance between the ligand and the receptors available on the endothelial cell surface. Our findings are also relevant to vascular remodeling in cancer, where context-dependent differences in the balance between the pro- and antiangiogenic actions of BMP9 could help to explain contrasting findings on the role for BMP9 in the vascularization certain tumor models.<sup>24,25,44</sup>

An important limitation of the current study is the absence of mechanistic data to explain how *BMPR-II* loss influences receptor-ligand interactions at the cell surface. Ligand-receptor interactions in the BMP/TGF $\beta$ /activin superfamily are complex and tightly controlled by the relative expression of a variety of type I and type II receptors, each with different affinities for their respective ligands. The abundance of *BMPR-II*, relative to other type II BMP receptors,<sup>45</sup> can greatly influence the sequestration of type-I receptors and BMP ligands through mechanisms that are independent of signaling via the receptor itself. Future work to explore this balance will require overexpression and deletion studies involving all 3 type II BMP receptors, *BMPR-II*, *ActR-IIa*, and *ActR-IIb*, either alone or in combination, to determine the precise ligand-receptor interactions through which BMP9 drives endothelial proliferation in the absence of *BMPR-II*.

Moving forward, our findings could have implications for the translation of recombinant BMP9 to the clinic as a novel PAH therapy. If individuals who exhibit substantially reduced *BMPR-II* levels are susceptible to excessive endothelial proliferation in response to recombinant BMP9 treatment, a strategy that involves the stratification of patients based on *BMPR-II* expression in cultured BOECs may be required to identify individuals who would benefit from this therapeutic approach, versus those for whom BMP9 administration could prove to be counterproductive. Moreover, recent studies have identified retinal vascular tortuosity as a marker of systemic vascular disease in the PAH patient population.<sup>46</sup> This finding raises the possibility of screening potential subjects for

BMP9 therapy based on their retinal vascular structure. Such considerations may appear cumbersome but could help to navigate the heterogeneity in the PAH patient population.

## ARTICLE INFORMATION

Received August 19, 2019; accepted September 11, 2020.

### Affiliations

Departments of Biomedical and Molecular Sciences (A.L.T., L.G.H., L.R.H., M.K.M.W., D.V.C., J.L.M., D.H.M., M.L.O.), Medicine (K.J.D.-S., J.M., P.D.J., S.L.A., M.L.O.), and Surgery (M.L.O.), Queen's University, Kingston, Canada.

### Acknowledgments

All pulmonary arterial hypertension patient blood outgrowth endothelial cell lines, and a subset of the healthy control lines, were generated by M.L. Ormiston in the laboratory of Prof Nicholas Morrell (University of Cambridge, Cambridge, United Kingdom). Work was performed in partnership with the Queen's Cardiopulmonary Unit.

### Sources of Funding

This study was supported by the Canadian Institutes of Health Research (PJT-152916) and the Ontario Thoracic Society.

### Disclosures

None.

## REFERENCES

1. Michelakis ED. Pulmonary arterial hypertension: yesterday, today, tomorrow. *Circ Res*. 2014;115:109–114. doi: 10.1161/CIRCRESAHA.115.301132
2. Morrell NW, Adnot S, Archer SL, Dupuis J, Jones PL, MacLean MR, McMurtry IF, Stenmark KR, Thistlethwaite PA, Weissmann N, et al. Cellular and molecular basis of pulmonary arterial hypertension. *J Am Coll Cardiol*. 2009;54(1 suppl):S20–S31. doi: 10.1016/j.jacc.2009.04.018
3. Lane KB, Machado RD, Pauciulo MW, Thomson JR, Phillips JA III, Loyd JE, Nichols WC, Trembath RC; International PPH Consortium. Heterozygous germline mutations in *BMPR2*, encoding a TGF-beta receptor, cause familial primary pulmonary hypertension. *Nat Genet*. 2000;26:81–84. doi: 10.1038/79226
4. Cogan JD, Pauciulo MW, Batchman AP, Prince MA, Robbins IM, Hedges LK, Stanton KC, Wheeler LA, Phillips JA III, Loyd JE, et al. High frequency of *BMPR2* exonic deletions/duplications in familial pulmonary arterial hypertension. *Am J Respir Crit Care Med*. 2006;174:590–598. doi: 10.1164/rccm.200602-1650C
5. Humbert M, Sitbon O, Chaouat A, Bertocchi M, Habib G, Gressin V, Yaici A, Weitzenblum E, Cordier JF, Chabot F, et al. Pulmonary arterial hypertension in France: results from a national registry. *Am J Respir Crit Care Med*. 2006;173:1023–1030. doi: 10.1164/rccm.200510-1668OC
6. Badesch DB, Raskob GE, Elliott CG, Krichman AM, Farber HW, Frost AE, Barst RJ, Benza RL, Liou TG, Turner M, et al. Pulmonary arterial hypertension: baseline characteristics from the REVEAL Registry. *Chest*. 2010;137:376–387. doi: 10.1378/chest.09-1140
7. Sztrymf B, Coulet F, Girerd B, Yaici A, Jais X, Sitbon O, Montani D, Souza R, Simonneau G, Soubrier F, et al. Clinical outcomes of pulmonary arterial hypertension in carriers of *BMPR2* mutation. *Am J Respir Crit Care Med*. 2008;177:1377–1383. doi: 10.1164/rccm.200712-1807OC
8. Atkinson C, Stewart S, Upton PD, Machado R, Thomson JR, Trembath RC, Morrell NW. Primary pulmonary hypertension is associated with reduced pulmonary vascular expression of type II bone morphogenetic protein receptor. *Circulation*. 2002;105:1672–1678. doi: 10.1161/01.cir.0000012754.72951.3d
9. Lavoie JR, Ormiston ML, Perez-Iratxeta C, Courtman DW, Jiang B, Ferrer E, Caruso P, Southwood M, Foster WS, Morrell NW, et al. Proteomic analysis implicates translationally controlled tumor protein as a novel mediator of occlusive vascular remodeling in pulmonary arterial hypertension. *Circulation*. 2014;129:2125–2135. doi: 10.1161/CIRCULATIONAHA.114.008777
10. Hopper RK, Moonen JR, Diebold I, Cao A, Rhodes CJ, Tojais NF, Hennigs JK, Gu M, Wang L, Rabinovitch M. In pulmonary arterial hypertension, reduced *BMPR2* promotes endothelial-to-mesenchymal transition

- via HMGA1 and its target slug. *Circulation*. 2016;133:1783–1794. doi: 10.1161/CIRCULATIONAHA.115.020617
11. Long L, Ormiston ML, Yang X, Southwood M, Gräf S, Machado RD, Mueller M, Kinzel B, Yung LM, Wilkinson JM, et al. Selective enhancement of endothelial BMPR-II with BMP9 reverses pulmonary arterial hypertension. *Nat Med*. 2015;21:777–785. doi: 10.1038/nm.3877
  12. Reynolds AM, Holmes MD, Danilov SM, Reynolds PN. Targeted gene delivery of BMPR2 attenuates pulmonary hypertension. *Eur Respir J*. 2012;39:329–343. doi: 10.1183/09031936.00187310
  13. Spiekerkoetter E, Tian X, Cai J, Hopper RK, Sudheendra D, Li CG, El-Bizri N, Sawada H, Haghghat R, Chan R, et al. FK506 activates BMPR2, rescues endothelial dysfunction, and reverses pulmonary hypertension. *J Clin Invest*. 2013;123:3600–3613. doi: 10.1172/JCI65592
  14. Toshner M, Voswinckel R, Southwood M, Al-Lamki R, Howard LS, Marchesan D, Yang J, Suntharalingam J, Soon E, Exley A, et al. Evidence of dysfunction of endothelial progenitors in pulmonary arterial hypertension. *Am J Respir Crit Care Med*. 2009;180:780–787. doi: 10.1164/rccm.200810-1662OC
  15. Caruso P, Dunmore BJ, Schlosser K, Schoors S, Dos Santos C, Perez-Iratxeta C, Lavoie JR, Zhang H, Long L, Flockton AR, et al. Identification of microRNA-124 as a major regulator of enhanced endothelial cell glycolysis in pulmonary arterial hypertension via PTBP1 (polypyrimidine tract binding protein) and pyruvate kinase M2. *Circulation*. 2017;136:2451–2467. doi: 10.1161/CIRCULATIONAHA.117.028034
  16. Diebold I, Hennigs JK, Miyagawa K, Li CG, Nickel NP, Kaschwich M, Cao A, Wang L, Reddy S, Chen PI, et al. BMPR2 preserves mitochondrial function and DNA during reoxygenation to promote endothelial cell survival and reverse pulmonary hypertension. *Cell Metab*. 2015;21:596–608. doi: 10.1016/j.cmet.2015.03.010
  17. Teichert-Kuliszewska K, Kutryk MJ, Kuliszewski MA, Karoubi G, Courtman DW, Zucco L, Granton J, Stewart DJ. Bone morphogenetic protein receptor-2 signaling promotes pulmonary arterial endothelial cell survival: implications for loss-of-function mutations in the pathogenesis of pulmonary hypertension. *Circ Res*. 2006;98:209–217. doi: 10.1161/01.RES.0000200180.01710.e6
  18. Beppu H, Ichinose F, Kawai N, Jones RC, Yu PB, Zapol WM, Miyazono K, Li E, Bloch KD. BMPR-II heterozygous mice have mild pulmonary hypertension and an impaired pulmonary vascular remodeling response to prolonged hypoxia. *Am J Physiol Lung Cell Mol Physiol*. 2004;287:L1241–L1247. doi: 10.1152/ajplung.00239.2004
  19. Hong KH, Lee YJ, Lee E, Park SO, Han C, Beppu H, Li E, Raizada MK, Bloch KD, Oh SP. Genetic ablation of the BMPR2 gene in pulmonary endothelium is sufficient to predispose to pulmonary arterial hypertension. *Circulation*. 2008;118:722–730. doi: 10.1161/CIRCULATIONAHA.107.736801
  20. David L, Mallet C, Keramidas M, Lamandé N, Gasc JM, Dupuis-Girod S, Plauchy H, Feige JJ, Bailly S. Bone morphogenetic protein-9 is a circulating vascular quiescence factor. *Circ Res*. 2008;102:914–922. doi: 10.1161/CIRCRESAHA.107.165530
  21. David L, Mallet C, Mazerbourg S, Feige JJ, Bailly S. Identification of BMP9 and BMP10 as functional activators of the orphan activin receptor-like kinase 1 (ALK1) in endothelial cells. *Blood*. 2007;109:1953–1961. doi: 10.1182/blood-2006-07-034124
  22. Herrera B, García-Álvarez M, Cruz S, Walsh P, Fernández M, Roncero C, Fabregat I, Sánchez A, Inman GJ. BMP9 is a proliferative and survival factor for human hepatocellular carcinoma cells. *PLoS One*. 2013;8:e69535. doi: 10.1371/journal.pone.0069535
  23. Herrera B, van Dinther M, Ten Dijke P, Inman GJ. Autocrine bone morphogenetic protein-9 signals through activin receptor-like kinase-2/Smad1/Smad4 to promote ovarian cancer cell proliferation. *Cancer Res*. 2009;69:9254–9262. doi: 10.1158/0008-5472.CAN-09-2912
  24. Cunha SI, Pardali E, Thorikay M, Anderberg C, Hawinkels L, Goumans MJ, Seehra J, Heldin CH, ten Dijke P, Pietras K. Genetic and pharmacological targeting of activin receptor-like kinase 1 impairs tumor growth and angiogenesis. *J Exp Med*. 2010;207:85–100. doi: 10.1084/jem.20091309
  25. Suzuki Y, Ohga N, Morishita Y, Hida K, Miyazono K, Watabe T. BMP-9 induces proliferation of multiple types of endothelial cells *in vitro* and *in vivo*. *J Cell Sci*. 2010;123(pt 10):1684–1692. doi: 10.1242/jcs.061556
  26. Yung LM, Nikolic I, Paskin-Flierlage SD, Pearsall RS, Kumar R, Yu PB. A selective transforming growth factor- $\beta$  ligand trap attenuates pulmonary hypertension. *Am J Respir Crit Care Med*. 2016;194:1140–1151. doi: 10.1164/rccm.201510-1955OC
  27. Tu L, Desroches-Castan A, Mallet C, Guyon L, Cumont A, Phan C, Robert F, Thuillet R, Bordenave J, Sekine A, et al. Selective BMP-9 inhibition partially protects against experimental pulmonary hypertension. *Circ Res*. 2019;124:846–855. doi: 10.1161/CIRCRESAHA.118.313356
  28. Ormiston ML, Toshner MR, Kiskin FN, Huang CJ, Groves E, Morrell NW, Rana AA. Generation and culture of blood outgrowth endothelial cells from human peripheral blood. *J Vis Exp*. 2015;106:53384.
  29. Marsboom G, Wietholt C, Haney CR, Toth PT, Ryan JJ, Morrow E, Thenappan T, Bache-Wiig P, Piao L, Paul J, et al. Lung <sup>18</sup>F-fluorodeoxyglucose positron emission tomography for diagnosis and monitoring of pulmonary arterial hypertension. *Am J Respir Crit Care Med*. 2012;185:670–679. doi: 10.1164/rccm.201108-1562OC
  30. Livak KJ, Schmittgen TD. Analysis of relative gene expression data using real-time quantitative PCR and the 2<sup>-</sup>(Delta Delta C(T)) Method. *Methods*. 2001;25:402–408. doi: 10.1006/meth.2001.1262
  31. Park SO, Lee YJ, Seki T, Hong KH, Fliess N, Jiang Z, Park A, Wu X, Kaartinen V, Roman BL, et al. ALK5- and TGFBR2-independent role of ALK1 in the pathogenesis of hereditary hemorrhagic telangiectasia type 2. *Blood*. 2008;111:633–642. doi: 10.1182/blood-2007-08-107359
  32. Beppu H, Lei H, Bloch KD, Li E. Generation of a floxed allele of the mouse BMP type II receptor gene. *Genesis*. 2005;41:133–137. doi: 10.1002/gene.20099
  33. Madisen L, Zwingman TA, Sunkin SM, Oh SW, Zariwala HA, Gu H, Ng LL, Palmiter RD, Hawrylycz MJ, Jones AR, et al. A robust and high-throughput Cre reporting and characterization system for the whole mouse brain. *Nat Neurosci*. 2010;13:133–140. doi: 10.1038/nn.2467
  34. Carpentier G. Angiogenesis analyzer. *Image J News*. 2012.
  35. Upton PD, Davies RJ, Trembath RC, Morrell NW. Bone morphogenetic protein (BMP) and activin type II receptors balance BMP9 signals mediated by activin receptor-like kinase-1 in human pulmonary artery endothelial cells. *J Biol Chem*. 2009;284:15794–15804. doi: 10.1074/jbc.M109.002881
  36. Zebedee Z, Hara E. Id proteins in cell cycle control and cellular senescence. *Oncogene*. 2001;20:8317–8325. doi: 10.1038/sj.onc.1205092
  37. Lo RS, Massagué J. Ubiquitin-dependent degradation of TGF-beta-activated smad2. *Nat Cell Biol*. 1999;1:472–478. doi: 10.1038/70258
  38. Cowburn AS, Crosby A, Macias D, Branco C, Colaco RD, Southwood M, Toshner M, Crotty Alexander LE, Morrell NW, Chilvers ER, et al. Hif2alpha-arginase axis is essential for the development of pulmonary hypertension. *Proc Natl Acad Sci USA*. 2016;113:8801–8806.
  39. Lee HW, Chong DC, Ola R, Dunworth WP, Meadows S, Ka J, Kaartinen VM, Qyang Y, Cleaver O, Bautch VL, et al. Alk2/ACVR1 and Alk3/BMPR1A provide essential function for bone morphogenetic protein-induced retinal angiogenesis. *Arterioscler Thromb Vasc Biol*. 2017;37:657–663. doi: 10.1161/ATVBAHA.116.308422
  40. Jakkula M, Le Cras TD, Gebb S, Hirth KP, Tuder RM, Voelkel NF, Abman SH. Inhibition of angiogenesis decreases alveolarization in the developing rat lung. *Am J Physiol Lung Cell Mol Physiol*. 2000;279:L600–L607. doi: 10.1152/ajplung.2000.279.3.L600
  41. Long L, Crosby A, Yang X, Southwood M, Upton PD, Kim DK, Morrell NW. Altered bone morphogenetic protein and transforming growth factor-beta signaling in rat models of pulmonary hypertension: potential for activin receptor-like kinase-5 inhibition in prevention and progression of disease. *Circulation*. 2009;119:566–576. doi: 10.1161/CIRCULATIONAHA.108.821504
  42. Song Y, Jones JE, Beppu H, Keane JF Jr, Loscalzo J, Zhang YY. Increased susceptibility to pulmonary hypertension in heterozygous BMPR2-mutant mice. *Circulation*. 2005;112:553–562. doi: 10.1161/CIRCULATIONAHA.104.492488
  43. Tian W, Jiang X, Sung YK, Shuffle E, Wu TH, Kao PN, Tu AB, Dorfmueller P, Cao A, Wang L, et al. Phenotypically silent bone morphogenetic protein receptor 2 mutations predispose rats to inflammation-induced pulmonary arterial hypertension by enhancing the risk for neointimal transformation. *Circulation*. 2019;140:1409–1425. doi: 10.1161/CIRCULATIONAHA.119.040629
  44. Porcù E, Maule F, Boso D, Rampazzo E, Barbieri V, Zuccolotto G, Rosato A, Frasson C, Viola G, Della Puppa A, et al. BMP9 counteracts the tumorigenic and pro-angiogenic potential of glioblastoma. *Cell Death Differ*. 2018;25:1808–1822. doi: 10.1038/s41418-018-0149-9
  45. Upton PD, Long L, Trembath RC, Morrell NW. Functional characterization of bone morphogenetic protein binding sites and Smad1/5 activation in human vascular cells. *Mol Pharmacol*. 2008;73:539–552. doi: 10.1124/mol.107.041673
  46. Nickel NP, de Jesus Perez V, Dubra A, Zamanian RT. Retinal vascular tortuosity, a new feature of systemic manifestation of pulmonary arterial hypertension. *Am J Respir Crit Care Med*. 2019;199:A5592.